

Laser-Induced Decomposition of NTO

Nancy L. Garland,* H. D. Ladouceur, and H. H. Nelson

Chemistry Division, Code 6110, Naval Research Laboratory, Washington, D.C. 20375-5342

Received: June 25, 1997[⊗]

The initial decomposition products of 3-nitro-1,2,4-triazol-5-one (NTO) are characterized using laser-induced decomposition of a solid sample. Heating of solid NTO samples is achieved by irradiation with 7 ns pulses of 266 nm laser light while the gas-phase products are detected using 118 nm single-photon ionization in a time-of-flight mass spectrometer. Product translational temperatures and relative product yields are obtained by analysis of time-of-arrival scans. The translational temperature depends linearly on decomposition laser fluence and agrees with the results of a calculation of the temperature rise in the irradiated volume using the heat conduction equation. The relative product yields are used to determine the percent decomposition of NTO as a function of temperature. The temperature dependence of the experimental fractional decomposition is consistent with that obtained from an RRKM calculation of the temperature dependence of NTO unimolecular decomposition. The temperature dependence of the relative product yields is used to identify the initial channels. The initial reaction appears to be bimolecular with a net loss of an O atom to yield nitroso-TO. Early unimolecular reactions include loss of NO₂ and nitro–nitrite rearrangement followed by loss of NO.

Introduction

NTO (3-nitro-1,2,4-triazol-5-one) is a relatively new energetic material with the attractive characteristics of relatively low sensitivity and potential high performance.¹ The insensitivity arises from a high barrier to reaction² and unusually stable initial decomposition products. A high heat of reaction (>77 kcal mol⁻¹)² and observation of autocatalytic behavior in thermal decomposition studies^{3,4} suggest that NTO may be a high-performance energetic material. Characterization of the rate parameters and reaction products of energetic material decomposition can lead to increased understanding of the relationship between structure, sensitivity, and performance. Since the decomposition reaction steps are temperature-, pressure-, and possibly phase-dependent, studies carried out under different experimental conditions have led to strong disagreement about the initial pathways.

Two different experimental approaches have been used to characterize NTO decomposition. Slow, thermal heating experiments yield information about rate-determining steps and ultimately the long-term stability of NTO while fast temperature-jump experiments yield information about initial and intermediate decomposition products. The reported values of the global kinetic parameters obtained from thermal heating experiments^{3–6} differ considerably. This disagreement was resolved by Williams and Brill,⁷ who proposed that the sublimation and decomposition processes were not always carefully isolated in the different experiments. A deuterium kinetic isotope effect^{3,4} was observed in several studies suggesting that H atom abstraction occurs on or before the rate-determining step.

Various experimental techniques have been used to identify NTO decomposition products in slow heating experiments. With EPR detection, Menapace et al.³ observed a hydroxy–nitroxide radical following ultraviolet irradiation of dilute solutions of NTO while Yi et al.⁵ concluded from NMR measurements that the acidic H atom is adjacent to the C–NO₂ group. Using infrared detection, Rothgery et al.² identified H₂O, NO, CO₂, CO, and N₂O as initial product gases and Prabhakaran et al.⁶

detected CO₂ and N₂O as the first gases evolved. In both experiments, NO₂ was generated subsequently. Prabhakaran et al.⁶ propose that C–NO₂ cleavage is probably rate-determining and that, while nitro–nitrite rearrangement is possible, their data do not support this latter step as rate-determining. Östmark et al.,⁸ using electron impact ionization mass spectrometry to detect gas-phase products of a heated solid sample, identified the parent, products corresponding to loss of NO₂ ($m/z = 83–85$) and ring fragments with $m/z = 40–50$. These same products were observed following CO₂-laser-induced decomposition of NTO.⁸ Oxley et al.⁹ analyzed the gas-phase products N₂ and N₂O of thermal decomposition of isotopically labeled NTO. Proposed decomposition steps include C–NO₂ scission and a migration of the nitro group from the carbon atom to a nitrogen atom followed by breakup of the ring.

Rapid heating techniques are used to characterize the initial pathways of NTO decomposition. Beard and Sharma¹⁰ subjected solid NTO samples to various types of impact (X-ray, shock, heat, drop weight). The gas-phase products, identified using mass spectrometry and XPS, include the parent NTO molecule and fragments corresponding to loss of O, loss of NO, and loss of NO₂. Brill and co-workers¹¹ rapidly heated NTO on a filament and identified gas-phase products using FTIR spectroscopy. They observe NO as the predominant product at lower pressures and CO₂ as the major product at higher pressure. NO₂ is only seen after a significant amount of reaction has occurred. They propose that high pressure enhances secondary reactions leading to degradation of the more reactive products. Wight and co-workers¹² irradiated layered films of NTO and an infrared absorber with the output of a CO₂ laser and detected products using FTIR. CO₂ is the only product observed when the CO₂ laser fluence is low; neither NO₂ nor HONO is detected. The initial step is proposed to be bimolecular with the carbonyl group on NTO interacting with the nitro group on a second NTO molecule. McMillen and co-workers¹³ studied the decomposition of NTO induced by shock, slow thermal heating, and UV laser heating. Gas-phase products were detected using single-photon ionization in a time-of-flight mass spectrometer. The only product from thermal decomposition has $m/z = 85$ (possibly triazolone, TO) while the prominent

* Corresponding author. e-mail: nancy.garland@nrl.navy.mil.

[⊗] Abstract published in *Advance ACS Abstracts*, October 1, 1997.

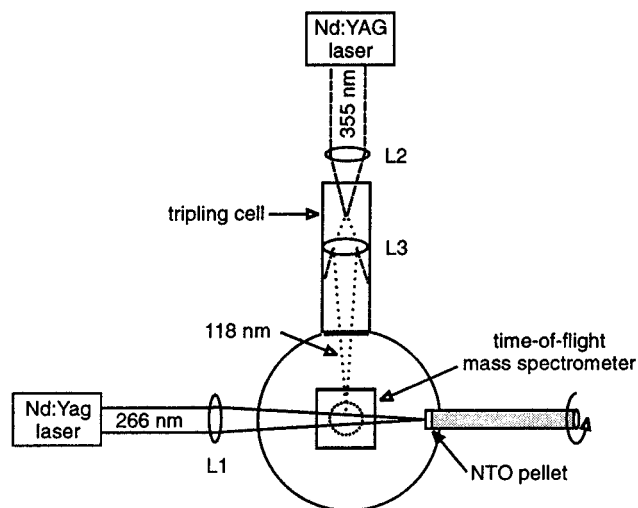


Figure 1. Schematic diagram of the experimental apparatus used in this work. The flight tube and mass spectrometer detector are perpendicular to the plane of the laser beams. L1 is a 30 cm focal length (f) fused silica lens, L2 is a 20 cm fl fused silica lens, and L3 is a 9.5 cm fl LiF lens.

products observed with laser-induced decomposition have $m/z = 114$ (nitroso-TO), 71, 43, and 30. Minor products include the fragments produced by loss of NO or NO₂. The proposed reaction scheme is nitro–nitrite rearrangement followed by loss of NO. Nitroso-TO ($m/z = 114$) is proposed to arise from addition of a radical R to the nitro oxygen followed by elimination of the RO group.

Clearly, there is considerable disagreement about the initial decomposition steps. H atom transfer has been identified as the rate-determining step.^{3,4} C–NO₂ bond cleavage was suggested as an initial step^{3,4,6} because the weakest bond in NTO is C–NO₂, but NO₂ has never been detected as an early evolved gas in any of the product studies. While nitro–nitrite rearrangement followed by loss of NO is observed in most of the rapid heating experiments, Wight and co-workers did not see NO in their thin-film studies. The energy required to break the N–O bond in the nitro group is greater than 83 kcal/mol¹³ so nitroso-TO ($m/z = 114$) is a product of a bimolecular rather than unimolecular reaction.

Information about the initial decomposition mechanism can be obtained by measuring the product yields as a function of temperature. In the present experiment, NTO is heated photothermally using laser irradiation of a solid sample. The use of pulsed lasers to desorb species rapidly from surfaces is a well-established analytical technique.^{14–17} The initial gas-phase products are identified using single-photon ionization and a time-of-flight mass spectrometer. Single-photon ionization avoids the complication of species fragmentation often encountered when using electron-impact ionization while mass spectrometry provides almost universal detection of the desorbed species. Time-of-arrival scans are used to determine the temperature of the sample surface and to obtain relative product yields.

Experimental Section

The experiments were carried out in a vacuum chamber with a time-of-flight mass spectrometer as illustrated in Figure 1. The NTO samples were prepared by pressing ~60 mg of NTO powder onto a KBr pellet. The pellets were epoxied to the end of the shaft of a rotating motor which is mounted on an XYZ translator attached to a flange of the vacuum chamber. Rotation of the pellet allows a fresh area to be sampled with each laser shot. The surface of the sample is approximately 4.8 cm from the center of the source region of the mass spectrometer.

NTO decomposition is achieved by focusing the 7 ns, 266 nm output of a Nd:YAG laser (Quantel 660-50) normal to the surface of the pellet. The pulse energy varied between 20 and 50 $\mu\text{J}/\text{pulse}$ with a spot size of $\sim 1 \times 10^{-4} \text{ cm}^2$, resulting in a fluence between 200 and 500 mJ cm^{-2} . Care was taken to ensure that the decomposition laser fluence was low enough such that ions were not produced directly at the surface.

After traveling to the ionization region of the mass spectrometer, neutral gas-phase products are ionized by a beam of 118 nm (10.5 eV) light directed perpendicular to the path of the decomposition laser. At this wavelength, most (but not all) products of NTO decomposition are ionized with a single photon. The low energy of the ionizing photons allows parent products to be detected without the complication of fragmentation as is observed with 70 eV electron-impact ionization. The 118 nm light is generated by frequency-tripling the 355 nm output of a Nd:YAG laser (Quantel 581-C) in a small, stainless steel cell containing a mixture of ~16 Torr of xenon and ~85 Torr of argon; the argon is added to achieve proper phase matching.¹⁸ The cell is attached to the vacuum chamber via a flange which contains a 9.5 cm focal length LiF lens which moderately focuses the 118 nm light through the ionization region (to improve mass resolution). The 355 nm beam is focused into the center of the tripling cell and diverges after the LiF lens.

The time-of-flight mass spectrometer is of the Wiley–McLaren design (R. M. Jordan Co.). Following the photoionization step, the ions are accelerated through a 0.89 m field-free flight tube and detected with a microchannel plate detector. To record a mass spectrum at a fixed time delay between the decomposition and ionization steps, the signal from the detector was captured by a digital storage oscilloscope (LeCroy 9400) and directed to a personal computer for data storage and analysis. Timing for the laser triggers is controlled by a digital delay generator (SRS DG-535) and a personal computer. Time-of-arrival scans of desorbed products after the decomposition laser pulse are obtained by monitoring the gated ion signal of a particular mass as the time delay between the two lasers is increased.

One possible complication in this experiment would be if the parent molecule is dissociatively ionized. One manifestation of dissociative ionization would be identical temporal distributions in the time-of-arrival scans of parent and daughter species which we do not observe. However, to confirm that dissociative ionization does not contribute to our observed ion signals, NTO was thermally decomposed in a Knudsen cell in the mass spectrometer, and the relative yields of the thermal decomposition products were monitored as a function of temperature. The Knudsen cell consisted of a glass tube with a small hole in one end in place of the rotating shaft; NTO crystals were placed in the end of the tube which was resistively heated with nichrome wire.

Results

A representative mass spectrum taken with a delay of 55 μs between the decomposition and photoionization lasers and a decomposition laser fluence of 380 mJ cm^{-2} is shown in Figure 2. As can be seen from the figure, at these decomposition laser conditions the NTO desorbed has undergone relatively little decomposition. A list of the major products observed in this spectrum and their proposed chemical formulas can be found in Table 1.

Translational and, as we will argue below, internal temperatures of the desorbed species can be obtained from time-of-arrival scans. A time-of-arrival scan of the parent NTO molecule taken with a desorption laser fluence of 350 mJ cm^{-2}

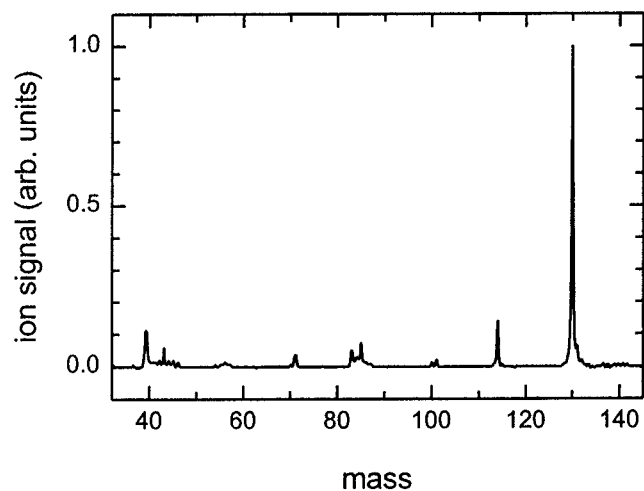


Figure 2. Time-of-flight mass spectrum of the products from NTO laser-induced decomposition. The decomposition laser fluence is 380 mJ cm^{-2} , and the delay between the decomposition and ionization lasers is $55 \mu\text{s}$.

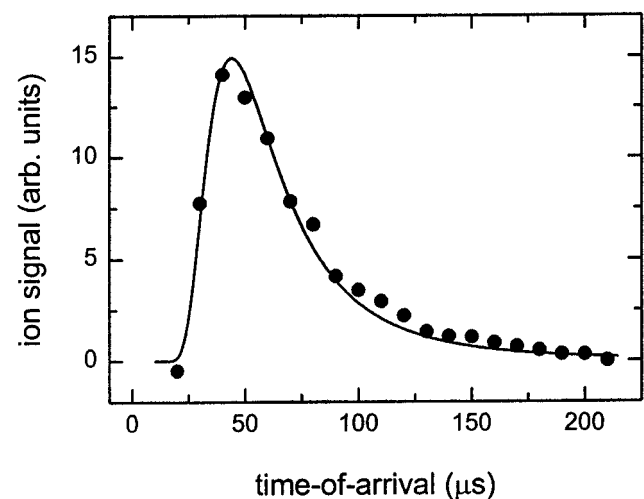


Figure 3. Time-of-arrival scan for the parent NTO molecule following laser desorption. The fluence of the decomposition laser is 350 mJ cm^{-2} . The points are experimental data, and the solid line is a fit to a thermal Maxwellian distribution with a translational temperature of $4700 \pm 300 \text{ K}$.

TABLE 1: Identification of Products following Laser-Induced Decomposition of NTO

obsd m/z	proposed product
27–30	HCN, ?, HCO, NO
42–46	NCO/CN ₂ H ₂ , HNCO, ?, ?, NO ₂
56	from 84?
71	CN ₃ OH
83–85	C ₂ N ₃ OH _x , $x = 1-3$
100	C ₂ N ₃ O ₂ H ₂
101	C ₂ N ₃ O ₂ H ₃
114	C ₂ N ₄ O ₂ H ₂
130	NTO, C ₂ N ₄ O ₃ H ₂

is shown in Figure 3. The solid line is a fit to a thermal Maxwellian distribution with a translational temperature of $4700 \pm 300 \text{ K}$. In a photothermal decomposition process, absorbed light energy is converted to internal and translational energy. The number of molecules that desorb and the translational energy of the products will depend on the number of photons whereas in a photochemical decomposition process only the number of desorbing molecules will depend on the number of photons. Figure 4 shows the dependence of the NTO translational temperature on desorption laser fluence. The linear correlation of the measured translational temperatures with

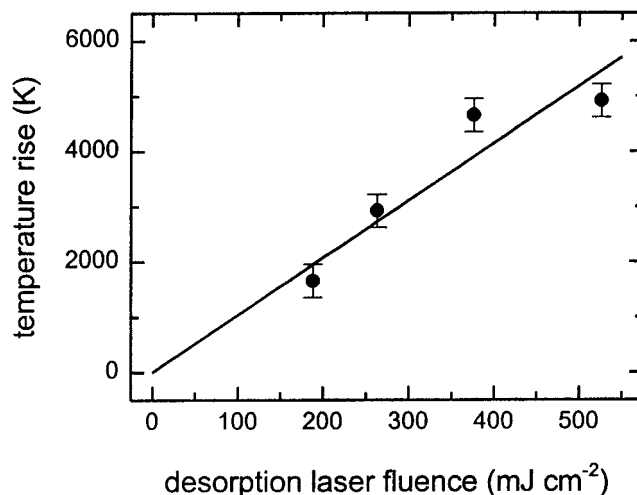


Figure 4. Translational temperature of NTO following laser desorption as a function of decomposition laser fluence. The points are temperatures calculated using thermal Maxwellian fits to time-of-arrival scans as described in the text. The solid line, which demonstrates the proportionality of translational temperature to laser fluence, is a fit to the data constrained to go through the origin.

desorption laser fluence is consistent with a photothermal mechanism. In addition, at a fixed decomposition laser fluence, the fitted translational temperatures of the different products observed are the same within experimental error. Since the products have molecular weights that differ by a factor of 1.5, the temporal distributions of the product time-of-arrival scans are different.

To characterize the initial decomposition steps, we focus on the higher molecular weight products since the lower molecular weight products observed, such as NO and NO₂, are more likely to result from a number of different secondary reactions, making the interpretation of their behavior difficult. Thus, we have measured the relative yields of products with $m/z = 114, 101, 85,$ and 83 as a function of temperature. The relative yield of a product is determined by velocity-weighting, to convert the measured species density to flux, and then integrating the ion signal of a time-of-arrival scan. No correction is made for the possible variation in the photoionization cross sections for the various products. The products yields are normalized by the velocity-weighted, integrated ion signal from the parent NTO molecule. Figure 5 is a plot of the relative product yields as a function of decomposition laser fluence for the four products mentioned.

Finally, to explore the possibility of dissociative ionization in the present experiments, thermal decomposition experiments were carried out in the mass spectrometer using the Knudsen oven described above. Because we only have pulsed ionization available in this apparatus, the signal-to-noise ratio in a continuous evolution experiment such as a Knudsen cell is greatly reduced from our normal, pulsed decomposition experiment. Nevertheless, the mass spectrum of effluent from the Knudsen oven showed NTO and products with $m/z = 83$ and 85 . As the temperature of the Knudsen oven was reduced, the relative intensities of the products decreased until, eventually, only ion signal from the parent molecule was detected, showing that dissociative ionization is not significant in this experiment.

Discussion

Before discussing the decomposition channels, the mechanism of production of hot NTO molecules in the present experiments is considered. Absorption of light from the 266 nm decomposition laser results in electronically excited NTO molecules.

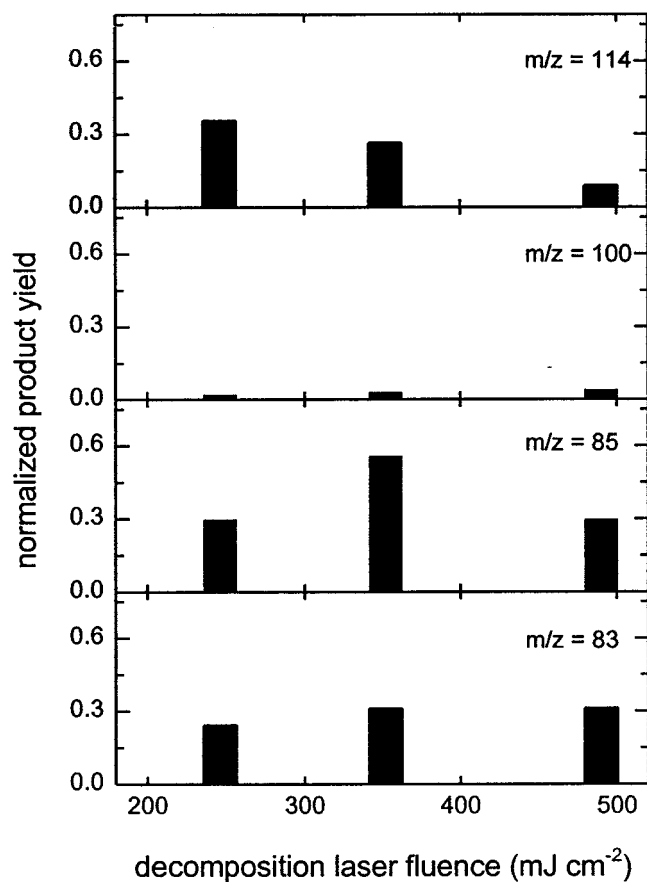


Figure 5. Normalized yields of NTO decomposition products as a function of decomposition laser fluence. Product yields are obtained by integration of the velocity-weighted time-of-arrival distribution of each product as described in the text. At each decomposition laser fluence, the product yields are normalized to the yield of NTO. We estimate an uncertainty of $\pm 20\%$ for each yield.

These excited molecules rapidly undergo internal conversion to the ground state from which decomposition occurs. There are two pieces of evidence to support this thermal mechanism. First, as discussed in the previous section, the observed translational temperature of desorbed NTO and all product species scales linearly with the desorption laser fluence. This is in contrast to expected constant translational energy if a photochemical mechanism was operative.¹⁹

Second, we have performed a calculation of the temperature expected for desorbing NTO molecules under each of our fluence conditions. The heat conduction equation²⁰ was used to estimate the temperature rise of the irradiated sample volume. The two-dimensional equation in cylindrical coordinates was solved numerically by a finite element code²¹ using the incident laser pulse energy, duration, and spot size, a heat capacity of $1.06 \text{ J g}^{-1} \text{ K}^{-1}$ and density of 1.9 g cm^{-3} , the thermal conductivity of HMX (in the absence of an extant value for NTO), and an absorption coefficient of $\sim 1.15 \times 10^4 \text{ cm}^{-1}$ at 266 nm (measured in our laboratory). The calculation assumes all the absorbed laser energy is converted to thermal energy. Temperatures calculated from the model are in good agreement with those obtained from the time-of-arrival scans as seen in Table 2. The close agreement between the calculated and observed translational temperatures is another confirmation of the thermal mechanism.

At first glance, it seems surprising that we observe any parent molecule from the NTO samples heated as high as 5000 K. The survival of the parent is easily understood, however, when one considers the short time duration of the experiment and

TABLE 2: Comparison of NTO Translational Temperature with Estimated Temperature Obtained Using the Heat Conduction Equation

fluence (mJ cm^{-2})	translational temp (K)	calculated temp (K)
188	1931	2313
263	3200	3121
376	4930	4337
526	5192	5952

the number of modes available in NTO. To check this notion, we have performed a simple RRKM calculation of the NTO unimolecular decomposition rate. The observed fractional decomposition is obtained by dividing the sum of the integrated product yields by the integrated total yield in the experiment as discussed in the last section. This can only be considered an order of magnitude estimate since we have not corrected for the expected variations in the photoionization cross section among the products at 10.5 eV. The calculation is performed using the UNIMOL suite of programs.²²

The input to the RRKM program includes temperature (obtained from the experimental time-of-arrival scans), critical energy (a bond strength of C-NO_2 of 70 kcal mol^{-1} is used²³), and vibrational frequencies adapted from ref 6 (experimental), ref 23 (calculated), and ref 24 (experimental and calculated). The program calculates the density of states $\rho(E)$ and the unimolecular rate constant $k(E)$ for energized NTO. The probability of a molecule having energy E is obtained by multiplying $\rho(E)$ by the Boltzmann factor. The probability of dissociation on the time scale of the experiment is estimated from $k(E)$. To determine the fraction of NTO molecules that dissociate at a particular temperature, the probability of a molecule having energy E is multiplied by the probability of dissociation, and the resulting distribution is integrated. The calculated percent decomposition increases from 3% at 2000 K to $>90\%$ at 4000 K while experimentally the percent decomposition increases from $\sim 20\%$ at 2000 K to $\sim 50\%$ at 4500 K.

The most direct information about initial decomposition steps comes from analysis of the decomposition laser fluence dependence of the higher molecular weight products since lower molecular weight products such as NO and NO_2 can arise from more than one reaction pathway. The high molecular weight products observed in this experiment arise from loss of O, loss of NO, and loss of NO_2 from NTO. These products are also seen in the laser-induced decomposition experiments of Beard and Sharma¹⁰ and McMillen et al.,¹³ but Beard and Sharma observed different relative yields. In their experiment, NTO is introduced into the mass spectrometer by heating the solid on a probe so the extent of thermal decomposition is not known. In addition, some fragmentation could occur in their mass spectrometer since either electron impact or chemical ionization of the products was used.

The translational temperature and the relative yields of the products depend on decomposition laser fluence as seen in Figures 4 and 5, respectively. In particular, Figure 5 shows the relative yield of the four major high molecular weight products as a function of decomposition laser fluence (internal temperature). The four fragments exhibit three different functional forms as the decomposition laser fluence is increased. Nitroso-TO is the most abundant observable product at the lowest laser fluence, and its yield decreases as the fluence (i.e., temperature) increases. (Since the photoionization cross sections of the fragments are not known, care must be taken when comparing the yields of different products at a given fluence.) This is the behavior expected for an initial decomposition product which then decomposes further as increased collisional

and secondary chemical processes become important at the higher temperatures. Thus, we propose that the initial step in NTO decomposition is the production of nitroso-TO. McMillen et al.¹³ have pointed out that this step is almost certainly bimolecular since the N–O bond strength is greater than 83 kcal/mol. This mechanism is also consistent with the results of Wight and co-workers,¹² who observe CO₂ (which we are unable to ionize at 118 nm) as an initial product and propose that it arises from the interaction of the carbonyl group on one NTO molecule with a nitro group on a second NTO.

The product with $m/z = 100$ corresponding to loss of NO is not observed at the lowest laser fluence, and its yield increases as the fluence is increased from 350 to 500 mJ cm⁻². The positive dependence of the yield on laser fluence suggests that this minor fragment is an early but not initial product. Likewise, the yield of the product with $m/z = 83$ corresponding to loss of HONO increases slightly as the laser fluence is increased; the positive temperature dependence of the yield suggests that this fragment is an early (but not initial) product.

The temperature dependence of the yield of the product with $m/z = 85$ corresponding to loss of NO₂ and gain of a hydrogen atom follows yet a third form; the yield appears to increase and then decrease with increasing laser fluence over the range 250–500 mJ cm⁻². This is the temperature dependence expected for a pathway that is increasingly accessible at high energies. As the temperature increases, however, the product undergoes decomposition or subsequent reaction. Thus, this fragment also appears to be an early but not initial product. McMillen et al.¹³ have speculated on production mechanisms for this fragment.

Summary

Solid samples of NTO decompose following irradiation with ultraviolet laser light. The decomposition products are identified using single-photon ionization in a time-of-flight mass spectrometer. Product translational temperatures are found to depend linearly on decomposition laser fluence, and the temperatures observed are consistent with calculations of the temperature assuming all laser energy is converted to heat. This suggests a photothermal decomposition process. The early reaction pathways are characterized by analysis of temperature dependence of the relative product yields. The initial product in this experiment is the fragment produced by net loss of an oxygen atom from NTO. This is consistent with earlier observations of CO₂ as an early product. Fragments produced by loss of NO and by scission of the C–NO₂ bond are early but not initial products.

Acknowledgment. We acknowledge the financial support of the Office of Naval Research through the Naval Research Laboratory. We thank Tom Russell of NRL for supplying the NTO samples and Tom Russell, Tod Botcher, Jeff Owrutsky, and Andy Baronavski of NRL for helpful discussions and Don McMillen and Jim Smith for providing copies of their manuscripts prior to publication.

References and Notes

- (1) Lee, K.-Y.; Chapman, L. B.; Coburn, M. D. *J. Energ. Mater.* **1987**, *5*, 27.
- (2) Rothgery, E. F.; Audette, D. E.; Wedlich, R. C.; Csejka, D. A. *Thermochim. Acta* **1991**, *185*, 235.
- (3) Menapace, J. A.; Marlin, J. E.; Bruss, D. R.; Dascher, R. V. *J. Phys. Chem.* **1991**, *95*, 5509.
- (4) Oxley, J. C.; Smith, J. L.; Zhou, Z.; McKenney, R. L. *J. Phys. Chem.* **1995**, *99*, 10383.
- (5) Yi, X.; Rongzu, H.; Xiyu, W.; Xiayun, F.; Chunhua, Z. *Thermochim. Acta* **1991**, *189*, 283.
- (6) Prabhakaran, K. V.; Naidu, S. R.; Kurian, E. M. *Thermochim. Acta* **1994**, *241*, 199.
- (7) Williams, G. K.; Brill, T. B. *J. Phys. Chem.* **1995**, *99*, 12536.
- (8) Östmark, H.; Bergman, H.; Åqvist, G. *Thermochim. Acta* **1993**, *213*, 165.
- (9) Oxley, J. C.; Smith, J. L.; Rogers, E.; Dong, X. X. *J. Phys. Chem. A* **1997**, *101*, 3531.
- (10) Beard, B. C.; Sharma, J. J. *J. Energ. Mater.* **1993**, *11*, 325.
- (11) Williams, G. K.; Palopoli, S. F.; Brill, T. B. *Combust. Flame* **1994**, *98*, 197.
- (12) Botcher, T. R.; Beardall, D. J.; Wight, C. A.; Fan, L.; Burkey, T. *J. Phys. Chem.* **1996**, *100*, 8802.
- (13) McMillen, D. F.; Erlich, D. C.; He, C.; Becker, C. H.; Shockey, D. A. *Combust. Flame*, submitted.
- (14) Nogar, N. S.; Estler, R. C.; Miller, C. M. *Anal. Chem.* **1985**, *57*, 2441.
- (15) Engelke, F.; Hahn, J. H.; Henke, W.; Zare, R. N. *Anal. Chem.* **1987**, *59*, 909.
- (16) Li, L.; Lubman, D. M. *Rev. Sci. Instrum.* **1988**, *59*, 557.
- (17) Nogar, N. S., Ed. *Laser Photoionization and Desorption Surface Analysis Techniques*; SPIE: Bellingham, WA, 1990; Vol. 1208.
- (18) Reintjes, J. F. *Nonlinear Optical Parametric Processes in Liquids and Gases*; Academic Press: Orlando, 1984; pp 49–58.
- (19) Cousins, L. M.; Leone, S. R. *Chem. Phys. Lett.* **1989**, *155*, 162.
- (20) Ozisik, M. N. In *Heat Conduction*; John Wiley: New York, 1980; p 83.
- (21) PDEase, available from Macsyma Inc., 20 Academy Street, Arlington, MA 02174.
- (22) Gilbert, R. G.; Smith, S. C.; Jordan, M. J. T. *UNIMOL program suite (calculation of fall-off curves for unimolecular and recombination reactions)*, 1993. Available from the authors: School of Chemistry, Sydney University, NSW 2006, Australia, or by E-mail to gilbert_r@summer.chem.su.oz.au.
- (23) Harris, N. J.; Lammertsma, K. *J. Am. Chem. Soc.* **1996**, *118*, 8048.
- (24) Sorescu, D. C.; Sutton, T. R. L.; Thompson, D. L.; Beardall, D.; Wight, C. A. *J. Mol. Struct. (THEOCHEM)* **1996**, *384*, 87.